IEEE Access
Multidisciplinary | Rapid Review | Open Access Journal

Received December 15, 2017, accepted January 15, 2018, date of publication March 5, 2018, date of current version March 16, 2018.

Digital Object Identifier 10.1109/ACCESS.2018.2804091

Flexible Convoluted Ring Shaped FSS for X-Band Screening Application

WAI YAN YONG[1], (Student Member, IEEE), SHARUL KAMAL ABDUL RAHIM[1], (Senior Member, IEEE), MOHAMED HIMDI[2], FAUZIAHANIM CHE SEMAN[3], (Member, IEEE), DING LIK SUONG[3,4], MUHAMMAD RIDDUAN RAMLI[1], AND HUSAMELDIN ABDELRAHMAN ELMOBARAK[1]

[1]Wireless Communication Center, Universiti Teknologi Malaysia, Johor Bahru 81310, Malaysia
[2]Institute of Electronics and Telecommunication of Rennes, University of Rennes 1, 35000 Rennes, France
[3]Research Center of Applied Electromagnetic, Universiti Tun Hussein Onn Malaysia, Parit Raja 86400, Malaysia
[4]RF Station Sdn Bhd, Petaling Jaya 47820, Malaysia

Corresponding author: Wai Yan Yong (warrenyong92@gmail.com)

This work was supported in part by UTM through RUG under Grant 4J213 and Grant 17H23, in part by MOHE Malaysia through FRGS under Grant 4F901 and Grant 4G617, and in part by PRGS under Grant 4L662.

ABSTRACT A flexible and low profile frequency selective surface (FSS) with bandstop behavior for *X*-band signals is demonstrated in this paper to support the demand of the flexible wireless communication devices in the today's market. The resonating element of the FSS is realized using the convoluted ring loop element that is inspired by the conventional ring loop element. An additional of four stubs are added at each 90° of the conventional ring loop to miniaturize its overall dimension. The convoluted ring loop FSS has reduced the overall dimension of the conventional ring shape FSS to 0.25 λ_0 with a reduction of 33%. The proposed FSS is developing by utilizing the flexible polyethylene terephthalate substrate with the measured thickness of 0.125 mm and dielectric constant of 2.7. From the simulated transmission response of the FSS, it shows that the proposed convoluted ring loop FSS with planar feature manages to provide a signal attenuation up to 37 dB at 10 GHz for both normal and oblique angle of incidence up to 45° at TE and TM polarization. For validation purpose, the prototype of the FSS is manufactured using the inkjet printing technique. The FSS is bent in a different manner, such as bending the array FSS with different radius and bending the unit cell convoluted ring FSS row by row, to examine the bending effect toward the transmission response performance. All the simulated results are compared with the measured results, and these results are in concurrence with each other. By having the conformal features, the employability of the FSS is enhanced whereby the proposed flexible FSS can be employed as the sub-reflector for wearable antenna and conformal shields for electromagnetic compatibility applications.

INDEX TERMS Frequency selective surface (FSS), EMI, shielding, filter, inkjet printing, silver nanoparticles ink, PET substrate, miniaturization, flexible.

I. INTRODUCTION

The proliferation of the smart devices such as smartphones, smartwatch, and tablet caused the exacerbates demand for high communication data rate services [1], [2]. One of the solutions to triumph over this situation is to employ a smaller cell size so that the bandwidth that can be used will be increased [1], [3], [4]. However, when the cell size used become smaller, it will result in the rapid multiplication of base station number and prompt to the higher concentration of electromagnetic interference (EMI). This phenomenon has led to concerns over EMI's implication towards human health, electronic equipment's performance and communication system security [5], [6]. Thus, it is crucial to mitigate the unwanted signals [6]. The conventional approach of utilizing the metallic enclosure and signal jammer is impractical in this cases as it is costly to be implemented [6]. An alternative solution such as utilizing the wire mesh or metal foil may be employed as EMI shield, to protect RF circuitry from electromagnetic radiation. However, this approach obstructs all transmissions [5]. To overwhelm the weakness of the traditional solution, the FSS is recommended in this paper.

FSSs are defined as a periodic array structure that trumped-up from either radiating or non-radiating elements which

allow the FSS present as either a band-pass filter or band-stop filter [7]. However, unlike microwave filters, the FSS is operating in the function of both frequency and angle of incidence [6]. Therefore, it is widely used as a spatial filter to shield the unwanted signal. Apart from that, FSS is also widely used as a reflector to improve antenna performance [8] and beam switching solution for antennas [9]. With such extensive application of FSS, compatibility with other devices and hassle-free installation within existing building and devices come into mind.

Recently, there has been a growing interest in developing flexible electronics. This trend is also happening in the wireless communication industry where the industries are looking for bendable antennas or microwave devices [10], [11]. One of the common approaches is to design the antennas and microwave devices on top of Polydimethylsiloxane (PDMS) [10], [12], [13]. Although PDMS is the best candidate to realize the flexible wireless devices, it is challenging to deposit the conductive element on top of it especially for the array types microwave devices such as FSS and reflect-array antenna. In order to deposit the conductive layer on the PDMS substrate, the pattern transfer manufacturing technique is employed [10], [13]. The proposed technique required the pattern of the conductive layer parts to be prior patterned using the cutter machine before it being transferred into the PDMS substrate. These technique is however impractical for the development of the array structure like FSS where number of array need to be patterned on the conductive patches and transfer into PDMS unit cell by unit cell which result in the labour intensive and inconsistency in the quality of the fabricated FSS such as alignment and dimension issues. On the other hand, developing of the conductive layer using inkjet printing to the PDMS is however unworkable due to the fact that PDMS having low low-adhesive surface, this phenomenon caused the ink deposited on the PDMS surface is become larger than the expected which will altered the resonat frequency of the FSS. To overcome these hindrance, development of the microwave devices on top of a paper substrate and Polyethylene Terephthalate (PET) using inkjet printing technique is then introduced [14]. However, there is a drawback in using these substrates as nanoparticles ink that deposited on the substrate using inkjet printing will only turn into conductive path after undergoes the thermal sintering process at high temperature for a long period of time [14]. To solve the mentioned weakness, the chemical sintering process is considered as it allows the nanoparticles ink turn into conductive within few seconds time [15].

In this paper, a single-band convoluted ring loop (CRL) FSS designed on the specially coated PET substrate to provide the screening for X-band signal is proposed. The overall thickness of the FSS is 0.128 mm with the unit cell size of 7.5 $\times$ 7.5 mm. The design exhibited good polarisation and angular stability performance with a -10 dB bandwidth of 38% in measurement at operating frequency of 10 GHz. In order to ensure the proposed FSS manage to operate reliably when it is bent, the semi-infinite simulation technique using CST MWS is proposed to evaluate the bending of the array FSS. To further enhance the employability of the proposed FSS, in this paper, we as well, investigate the bending effect of the row-by-row unit cell FSS. From both simulation and measurement results, the recommended FSS manage to provide a satisfactory performance when it is being bent in the mentioned manners. With these conformal features,the employability of the FSS is enhanced whereby the proposed flexible FSS can be employed as the sub-reflector for wearable antenna and conformal shields for EMC applications.

II. MATERIAL CHARACTERISATION

A. SILVER NANOPARTICLES INK

The silver nanoparticles ink named AgIC #1000 ink supplied from (AgIC, Japan) is composed of silver, water and ethanol with viscosity of around 2–3 mPa.s and surface tension around 30–35 mN/m [15]. The conductivity of the silver nanoparticle ink is examined through the electrical resistance using two probe measurement. The electrical resistance of single layer silver nanoparticles ink with thickness of ± 0.003 mm is around $\pm 0.3\ \Omega$/m. The conductivity of the silver nanoparticles ink, $\sigma_{Ag} = 5 \times 10^6$ S/m, was obtained from Equation (1)

$$\sigma_{Ag} = \frac{L}{RAc} \tag{1}$$

where R is electrical resistance, A_c is the cross sectional area and L is the length [14].

B. POLYETHYLENE TEREPHTHALATE (PET)

The specially coated PET substrate supplied by (AgIC, Japan) was characterized using open-ended coaxial probe with a vector network analyser of up to 13 GHz. An additional layer of chemical is deposited on top of PET substrate which allows the silver nanoparticles ink undergoes chemical sintering process when it is coated on top of PET substrate. The layer of chemical deposited on the PET substrate is the solvent that comprise of polymer latex and a halide emulsion, when the silver nanoparticle ink is deposited on it, the conductivity appears several seconds after the solution is dried. Therefore, the main advantage using these PET substrates supplied by (AgIC, Japan) is the silver nanoparticle ink turned into conductive ink within 3 seconds after being deposited. As such, fabrication period reduced drastically as compare to the thermal sintering process which takes up around 2 hours [14]. The measured dielectric constant of PET substrate was $\varepsilon_r = 2.7$ with the tangent lost was $tan\delta = 0.004$. The PET substrate used is semi-transparent as shown in Figure1. It also with flexible and highly elastic features [14].

III. ELEMENT DESIGN OF FSS

The recommended design of the FSS element is demonstrated as in Figure 2 by using the CRL. The CRL element is reshaped from the ring slot element by introducing slot to it. This approach has exacerbated the package density of the ring

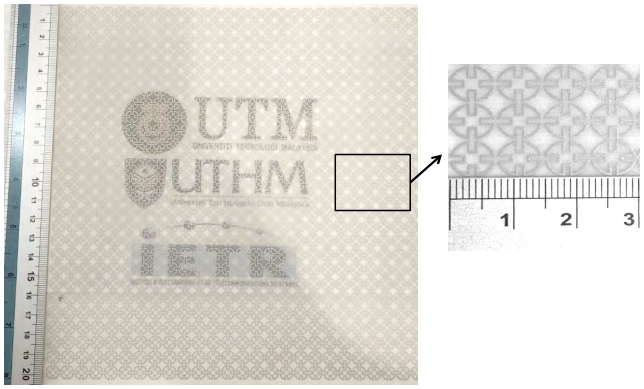

FIGURE 1. Fabricated CRL FSS on semi-transparent and flexible PET substrate.

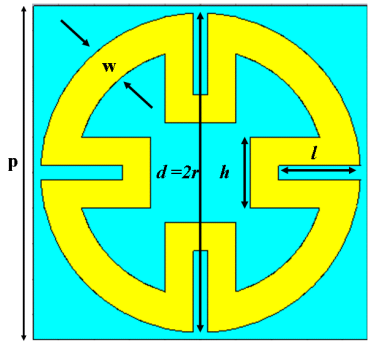

FIGURE 2. Unit cell of convoluted ring loop FSS; $p = 7.5mm$, $d = 7.2mm$, $h = 1.6mm$, $l = 1.2mm$, $w = 0.5mm$.

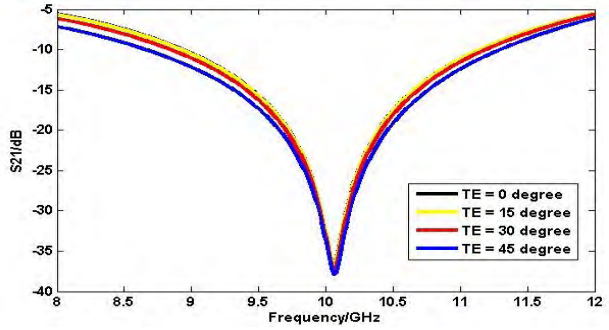

(a)

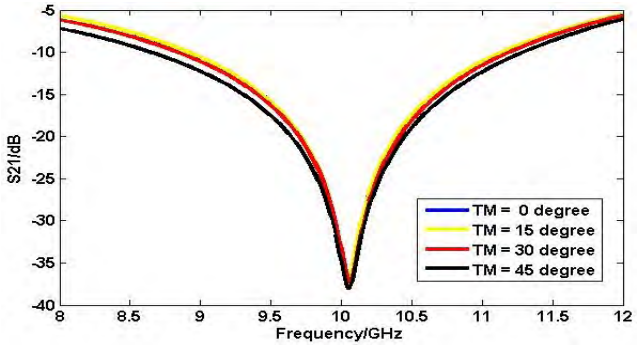

(b)

FIGURE 3. Simulated frequency response of (a) TE polarisation, (b) TM polarisation under various angle of incident.

loop element. By introducing the slot at each 90° of the conventional ring slot, the overall dimension of the unit cell has reduced by 33 %. Compact elements will further improve the performance of the FSS by offering a stable frequency response over a wide angle [6]. The proposed design is realized using silver nanoparticle ink and supported by a polyethylene terephthalate (PET) substrate with thickness, h of 0.125 mm and dielectric constant, ε_r of 2.7 with tangent loss of 0.004.

IV. SIMULATION RESULTS AND DISCUSSION

A. EVALUATION THE PERFORMANCE OF THE PLANAR FSS

The unit cell of the proposed ring slot FSS is simulated using Computer Simulation Technology (CST) Microwave Studio software. The simulation was done using the frequency domain solver as it is suitable for the simulation of a highly resonant structure as well as acknowledging the examination of the FSS performance with the variation of the angle of incident and polarization. The periodic boundary condition is set in both horizontal and vertical direction and z-direction is set to be open for locating the ports. To reduce the simulation load, CST full floquet port is utilized to simulate unit cell of FSS to model the proposed FSS as an infinite array in the CST simulation window. The simulated transmission response at the normal incident for both TE and TM polarisation of the proposed FSS is demonstrated in Figure 3. From Figure 3, it can be examined that at the normal incident the CRL provide signal attenuation up to 37 dB at 10 GHz. The proposed FSS provides a −10 dB bandwidth of around 23 %. Besides that, when the angle of incident increase up to 45° at the TE and TM polarisation, the frequency response of the FSS behaved almost the same. Therefore, it can be concluded that the CRL is insensitive toward the variation of the angle of incident and polarisations.

B. EVALUATION THE PERFORMANCE OF THE CONFORMAL FSS

In order to scrutinize the performance of the FSS when it is bent, Figure 4 illustrates the mechanism utilized to realize the conformal FSS. However, the aforementioned method which is the floquet port simulation is not directly applicable for the engineering-essential curved FSS as it is impractical to organize the FSS elements in a purely 2-D periodic sense when the FSS is bent. In order to evaluate the bending effect of the FSS array in the CST software, the unit cell simulation is not applicable as it will assume each and every single unit cell is bent. Thus, a finite model analysis is proposed in the evaluation of the bending effect of the FSS [16], but this required a heavy computational loading. Therefore, in this paper, a semi-infinite model is proposed in the evaluation of the bending of the FSS array.

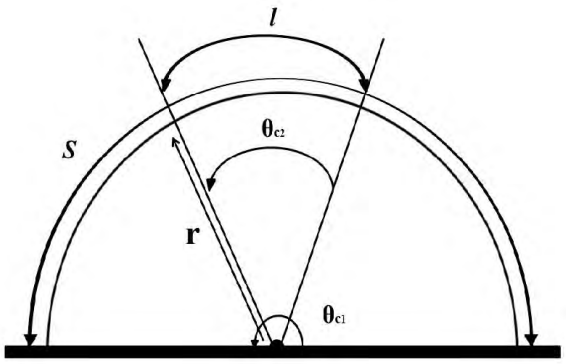

FIGURE 4. Model utilized for the development of the conformal FSS.

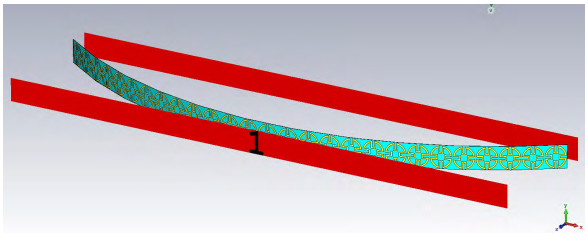

FIGURE 5. Simulation setup for the evaluation of the conformal FSS array using CST.

Figure 5 encapsulates the simulation set-up in CST that utilized for the examination of the performance of the conformal FSS array. As it can be observed from the figure, when the radius of the semi-cylinder, r is increase, the arc angle, θ_{c2} of the semi-cylinder will become larger. This phenomenon allow a wider arc of the bended structure can be obtained. The simulation of the conformal FSS array is completed by drawing a finite single row of the FSS array formed on a semicircle and the PEC or PMC boundary at the direction of the periodic array needed and open boundary at the bending direction or finite array is utilized for the simulation. By employing this simulation setup, it has significantly reduced the simulation efforts in the evaluation of the conformal FSS array as compared to the simulation of the full finite FSS structure. However, this technique only allows the investigation of the bending performance at normal incidence.

Figure 6 illustrates the comparison of the simulated transmission response of the planar FSS and the conformal FSS at the normal angle of incidence for TE polarization. From the simulated results, it can be observed that when the array of the FSS is bent at the different radius of the semi-cylinder, r, the resonant frequency is shifted from 10.1 GHz to 9.4 GHz with the alteration of 6.93%. In addition, the simulated result shows that the resonant frequency altered more significant when the FSS is bend at the radius of 150mm as compare to the 200mm. This is phenomenon can be understand from the Figure 4, when the radius of the semi-cylinder increase, the arc angle, θ_{C2} is also become wider which result in a less bending impact of the FSS. Thus the coupling effect among the elements and the change in the impedance of the

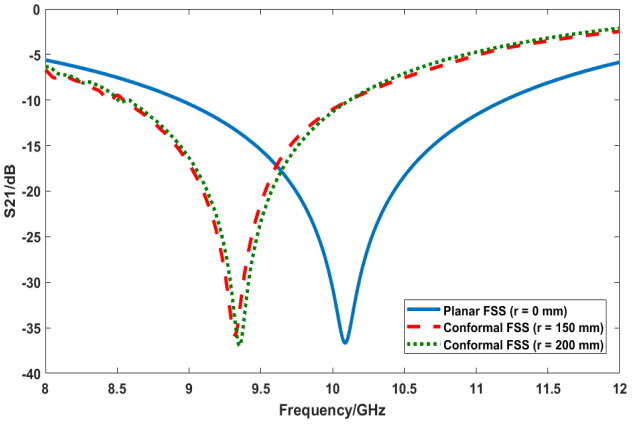

(a)

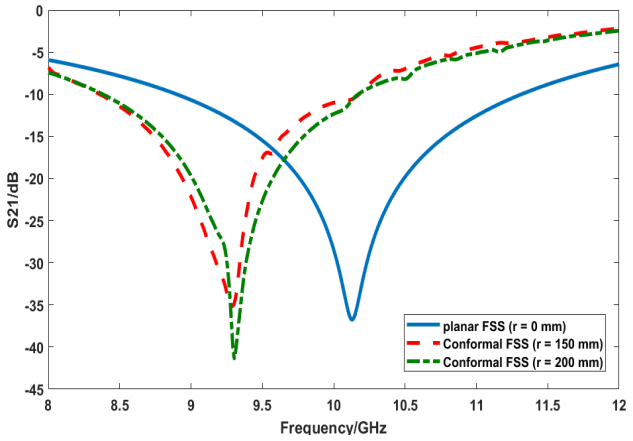

(b)

FIGURE 6. Comparison of the transmission response for planar and the conformal FSS array for (a) TE polarization and (b) TM polarization.

FSS is lesser as compare to smaller semi-cylinder radius. Consequently, it can be concluded that the shifting is the resonant frequency is inversely proportional to the radius of the bending. On the other hand, the bandwidth performance degraded significantly, whereby the bandwidth for the planar FSS is around 22.78% and reduced to only 14.89% when the FSS array is bent with a radius of 150 mm and 200 mm.

Apart from that, in order to study the bending effect toward the performance of the FSS, the unit cell of the FSS is bent row by row as illustrated in Figure 7. From the figure, it can be observed that each unit cell of the FSS is bent with a radius of 4mm in the x-direction and thus result in a row-by-row unit cell bending. The simulation setup employed to investigate the proposed conformal FSS structure is the conventional unit cell simulation set-up in the CST software. The unit cell of the FSS is bent with a radius of 4mm and the x-direction and y-direction is defined as unit cell, while z-direction is defined as open(add space). By employing this set-up the simulation loading is reduced significantly as compared to the full finite array simulation. Figure 8 exemplifies the simulated transmission response of the unit cell FSS with planar and conformal features for TE and TM polarization.

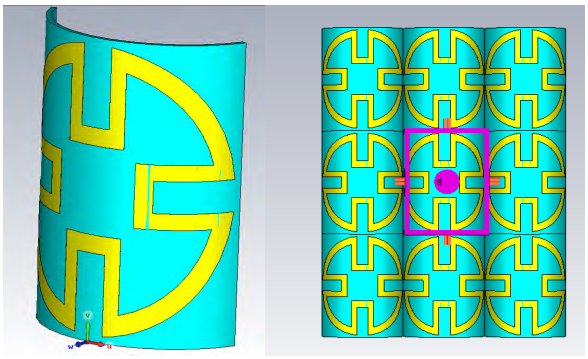

FIGURE 7. Bending of the row by row unit cell FSS.

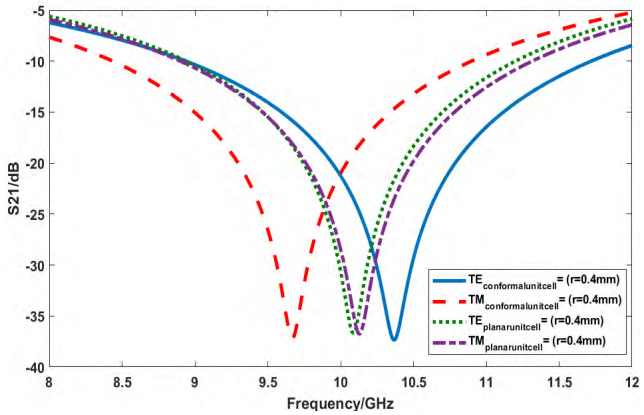

FIGURE 8. Simulated transmission response of the unit cell FSS with planar and conformal features for TE and TM polarization.

From the results, it can be contemplated that when the unit cell of the FSS is bent with a radius of 4mm, the resonant frequency is altered from 10 GHz to 10.4 GHz for TE polarization and from 10 GHz to 9.6 GHz for TM polarization. The shifting in the resonant frequency is mainly attributed to the variation of the impedance properties of the FSS as the coupling effect among the elements are changed when it is bent. Nevertheless, in term of the bandwidth performance, the bandwidth improved from 22.78% to 26.67% and 32.21 % for TE and TM polarization, respectively at normal incidence.

V. FABRICATION AND MEASUREMENT OF THE FSS PROTOTYPE

A. PLANAR FSS

In order to validate the proposed FSS experimentally, the designed FSS is fabricated utilizing the inkjet printing technique. The main limitation of the inkjet printing is that the smaller unit cell dimension of the FSS that can be fabricated is reliable on the printer resolution. In this case, the width of the unit cell FSS need to remain at a minimum of 0.5mm which is the smaller dimension that can be fabricated using Brother MFC-J430W printer. The silver nanoparticles ink is filled into a special cartridge to be integrated with the used of Brother MFC-J430W Printer, as displayed in Figure 9. Before printing the designed FSS, the printer is pre-set in

FIGURE 9. Brother MFC-J430W printer with special catridge filled with silver nanoparticles ink used for fabricate the FSS prototype.

order to ensure that best printing quality is selected and color mode is arranged as vivid. After completing all the setting, the designed FSS is fabricated in array form on top of the specially coated PET substrate. The prototype of the fabricated FSS is as shown in Figure 1. The overall dimension of the fabricated FSS is 190.1 mm $\times$ 190.1 mm with 27 elements $\times$27 elements.

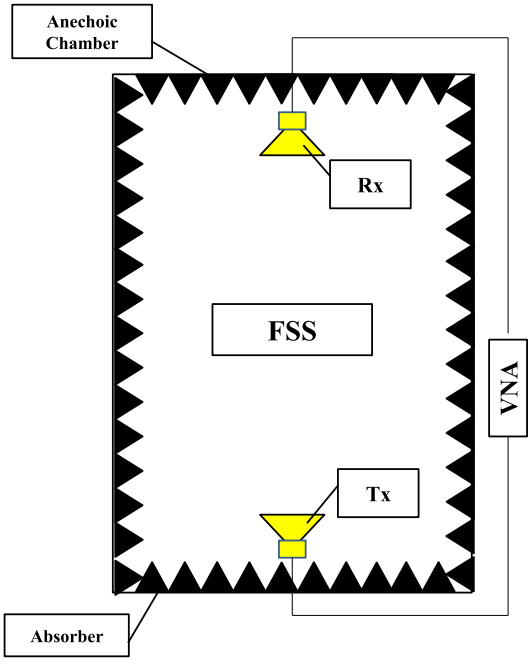

FIGURE 10. Measurement setup for FSS measurement.

Figure 10 illustrated the experimental setup to measure the transmission response of the FSS prototype for TE polarization. The measurement was carried out in the anechoic chamber. The measurement setup comprised of two horn antennas (transmitting and receiving antennas) which are connected to the Rohde & Schwarz Vector Network Analyzer using coaxial cables and the FSS prototype was placed in between of two horn antennas. The two horn antennas were placed at a distance of 60 cm away from each other to ensure the antennas

comply with far-field region theorem which is

$$d_{far-field} \geq 2D^2/\lambda \quad (2)$$

where $d_{far-field}$ is the minimum separation distance of two horn antennas, D is the maximum dimension of the antennas used and λ is the wavelength [6]. At the initial stage, the measurement was taken first without the FSS located in between the horn antennas to figure out the loss due to the propagation path. These losses are taken out later during the measurement of the FSS performance to make sure the attenuation of microwave signal entirely ascribed by the FSS prototype. The same procedures were repeated for the TM polarisation measurement with the exception that the horn antennas were rotated by 90°. A similar routine is followed by the measurement of the FSS performance at the various angle of incident, 15°, 30° and 45°.

The comparison of the simulated and the measurement results are presented in Figure 11. From the comparison results, it can be examined that the measurement results and the simulated results are coherent with each other. From Figure 11a, it can be observed that at 10 GHz, the FSS manage to provide the attenuation up to −35 dB for both TE and TM polarisation. Although the center frequency of the measured results is shifted slightly toward the lower frequency, this shifting of the frequency is acceptable. The shifting of the center frequency is mainly contributed from the fabrication errors caused by the resolution of the printer. When the angle of incident increase up to 45°, the center frequency of the measured results constantly remains at around 9.8 GHz with attenuation up 35 dB for both TE and TM polarization. On the other hand, at 10 GHz, the presented measured result show to have a minimum of 20 dB attenuation when the angle of incident is equal to 45°. Therefore, it can be concluded that the proposed FSS is insensitive towards the change in the angle of incident and polarisation of the incident waves. The insufficient graph smoothness is expected which is mainly contributed to the scattering effects of the electromagnetic waves experienced during the measurement and the edge reflections due to the conductive materials from the surroundings.

B. FLEXIBLE FSS

As discussed in the earlier section, the prototype of the flexible FSS is bent in two manners which are bending in array FSS form and bending in a row-by-row unit cell FSS. In this case, the bending of the array FSS is much uncomplicated as compared to the manufacturing process of the row-by-row unit cell FSS with conformal features. Figure 12 shows the measurement set-up that employed for the investigation of the transmission response of the conformal FSS finite array. It can be perceived from the figure, the finite array FSS prototype is attached to a semi-circular cylinder that made up from the foam that has the similar dielectric properties with the free space. By attaching the array FSS on the semi-circular cylinder foam, the prototype is bent according to it curvature. To obtain the measured transmission response

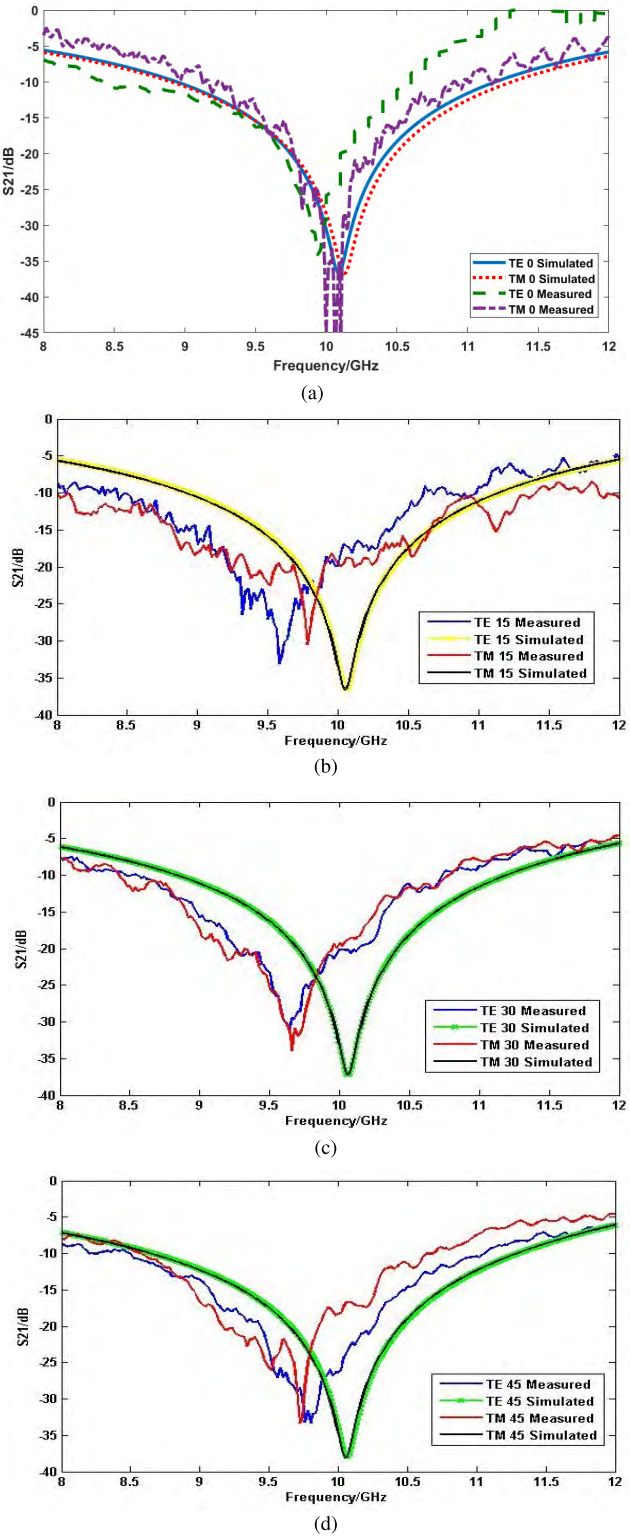

FIGURE 11. Comparison of the simulated and measured transmission response for TE and TM polarization at (a) $\theta = 0°$, (b) $\theta = 15°$, (c) $\theta = 30°$ and (d) $\theta = 45°$.

of the conformal array FSS, the similar routine used in the measurement of the planar FSS is repeated.

Figure 13 encapsulates the comparison of the simulated and measured transmission response for planar and

FIGURE 12. Experiment set-up used to evaluate the performance of the finite FSS array.

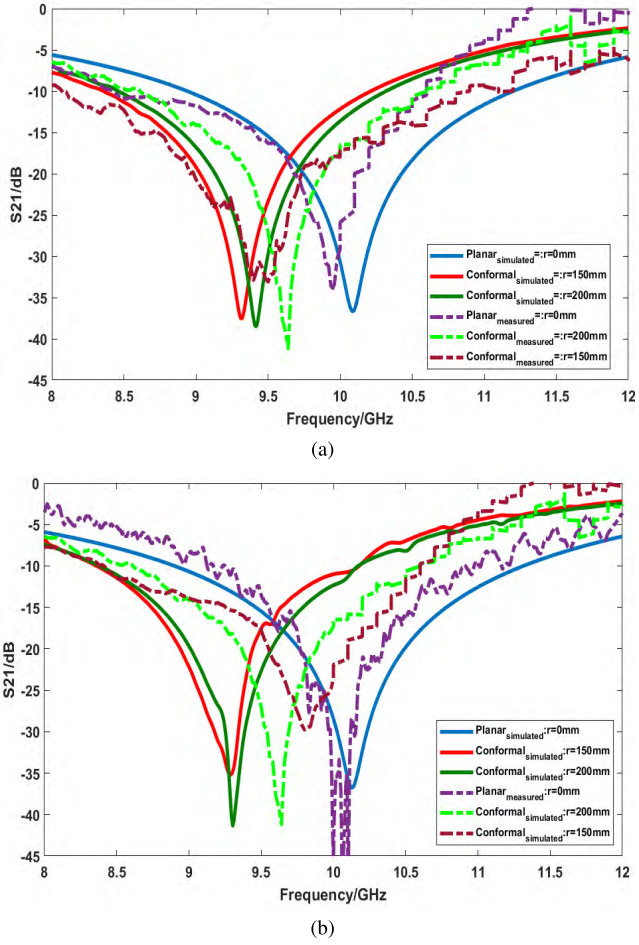

FIGURE 13. Comparison of the simulated and measured transmission response for the planar and conformal FSS array for (a) TE and (b) TM polarization.

conformal finite array FSS with the different radius of curvature for TE and TM polarization. It can be contemplated that, at both TE and TM polarization. It can be observed that, when the FSS array is bent with a radius of 150mm and 200mm, the resonant frequency is shifted to a lower frequency for both TE and TM polarization. This phenomenon is correspondences to the simulation results.

FIGURE 14. Aluminium mould employed for the bending of the row-by-row unit cell FSS.

On the other hand, the fabrication of the flexible row-by-row unit cell FSS is fabricated using an aluminum mold as illustrated in Figure 14. The finite FSS that fabricated on the PET substrate is attached to the aluminum mold and the covered is pressed on the PET-based FSS firmly for a period of time until the bending features are achieved. Figure 15 illustrates the fabricated row-by-row unit cell FSS. After the fabrication completed, the prototype of the FSS is measured using the two horn antenna connected to the vector network analyzer.

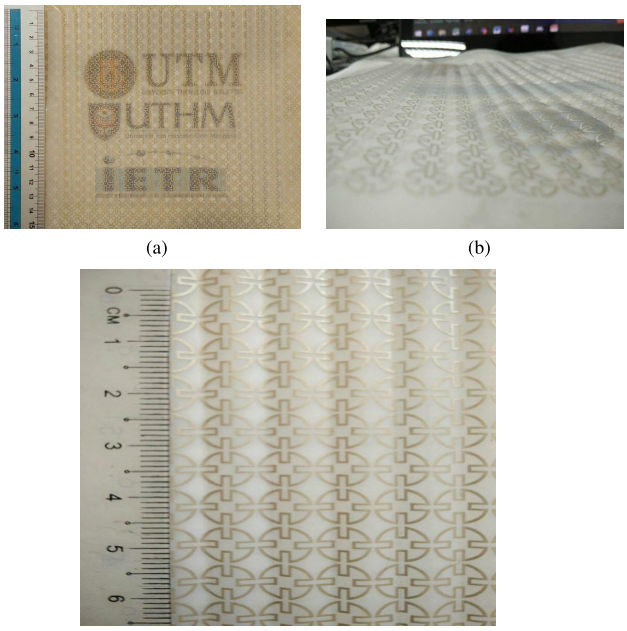

FIGURE 15. Fabricated row-by-row unit cell FSS prototype (a) top view, (b) side view, and (c) zoom view.

Figure 16 illustrates the comparison of the simulated and measured transmission response for the row-by-row unit cell FSS for TE and TM polarization at the normal angle of incidence. From the Figure 16a, it can be scrutinized that for TE polarization with normal angle, when the unit cell FSS is bent with a radius of 4mm, the measured resonant frequency is changed from 10 GHz to 10.5 GHz with a

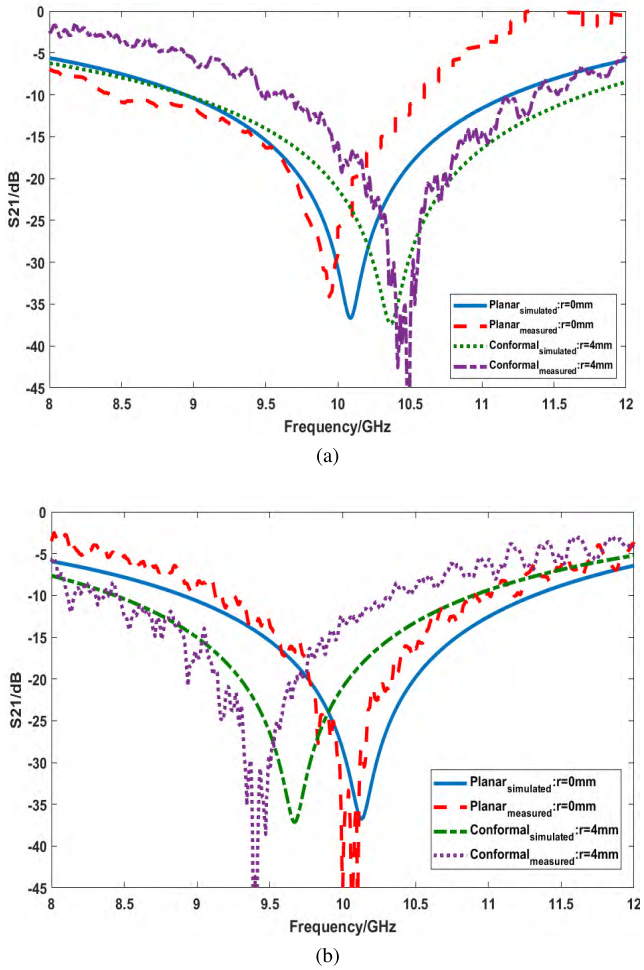

FIGURE 16. Comparison of the simulated and measured transmission response for the row-by-row unit cell FSS for (a) TE and (b) TM polarization at normal angle of incidence.

different of 5% which is in the good agreement with simulated results, whereby when the unit cell FSS is bent, the resonant frequency will altered to a higher frequency at TE polarization. On the other hand, for TM polarization as presented in Figure 16b, the simulated and measured results are shows that when the unit cell FSS is bent with a radius of 4mm, the center frequency is changed from 10 GHz to 9.4 GHz for simulation and to 9.6 GHz for measured results. It can be distinguished that, there is a shift of around 1-2% in between the simulation and measurement results. However, this slight alteration which is due to the imperfection occurs in the fabrication of the FSS. However, this slight shifting can be neglected. In general, for both TE and TM polarization, the simulated results and measured results for conformal row-by-row unit cell FSS are found to be in congruence with each other.

VI. CONCLUSION

A flexible and low-profile PET-based FSS for X-band signals screening is presented in this paper. The element of the proposed FSS is designed using the CRL elements which are modified from the ring loop element. The proposed design offers a minimum measured attenuation of 20 dB at the 10 GHz at the different angle of incidence and polarization. The CRL element has miniaturized the conventional ring loop element by around 33 %. This miniaturized element gives a credit for the angular independent operation up to 45° for both TE and TM polarisation. Besides that, the proposed FSS offers a low-profile with the overall thickness of 0.128 mm and unit cell dimension of 7.5 mm × 7.5 mm. A prototype of the proposed FSS is fabricated using the silver nanoparticles ink and the specially coated PET substrates supplied by AgIC and its performance is measured in the open area. Apart from that, to ensure the proposed FSS manages to operate substantially, the bending effect toward the flexible FSS is investigated in this paper. The proposed FSS is bent in two manners which are row-by-row unit cell bending and FSS array form bending. When FSS is bent in either manner, the resonant frequency is slightly shifted. The measured results are shown to have good agreement with the simulated results. Therefore, with the extraordinary performance in both planar and conformal features, the proposed FSS is suitable to employ as the sub-reflector for wearable antenna and conformal shields for EMC applications.. The future research will focus on the improvement of the bandwidth performance of the proposed FSS and enhance the compatibility toward bending effects of the FSS structure.

ACKNOWLEDGMENT

The authors would like to acknowledge to all members of Wireless Communication Center, UTM and The Institute of Electronics and Telecommunication of Rennes, IETR for their help and assistance in fabrication and measurement of the FSS prototype.

REFERENCES

[1] M. Agiwal, A. Roy, and N. Saxena, "Next generation 5G wireless networks: A comprehensive survey," *IEEE Commun. Surveys Tuts.*, vol. 18, no. 3, pp. 1617–1655, 3rd Quart., 2016.

[2] M. R. Ramli, S. K. A. Rahim, M. Idzam, and M. L. Samingan, "Performance analysis of microstrip grid array antenna on different substrates for 5G mobile communication," *J. Telecommun. Electron. Comput. Eng.*, vol. 8, no. 6, pp. 6–9, 2016.

[3] D. Muirhead, M. A. Imran, and K. Arshad, "A survey of the challenges, opportunities and use of multiple antennas in current and future 5G small cell base stations," *IEEE Access*, vol. 4, pp. 2952–2964, 2016. [Online]. Available: http://ieeexplore.ieee.org/lpdocs/epic03/wrapper.htm?arnumber=7470585

[4] D. Liu *et al.*, "User association in 5G networks: A survey and an outlook," *IEEE Commun. Surveys Tuts.*, vol. 18, no. 2, pp. 1018–1044, 2nd Quart. 2016.

[5] W. Y. Yong, S. K. A. Rahim, F. C. Seman, M. R. Ramli, and N. A. Remli, "Miniaturisation of ring shape element frequency selective surface for X-band shielding," in *Proc. IEEE Asia–Pacific Microw. Conf.*, Kuala Lumpur, Malaysia, Nov. 2017, pp. 877–880.

[6] F. C. Seman and N. K. Khalid, "Investigations on fractal square loop FSS at oblique incidence for GSM applications," in *Proc. Elect. Power, Electron., Commun., Control Inform. Seminar (EECCIS), Conjunct 1st Joint Conf. (UB-UTHM)*, Aug. 2014, pp. 62–66.

[7] R. J. Marhefka and J. D. Kraus, *Antennas For All Applications*, 3rd ed. New York, NY, USA: McGraw-Hill, 2003.

[8] X. Song, Z. Yan, T. Zhang, C. Yang, and R. Lian, "Triband frequency-selective surface as subreflector in Ku-, K-, and Ka-bands," *IEEE Antennas Wireless Propag. Lett.*, vol. 15, pp. 1869–1872, 2016.

[9] M. Bouslama, M. Traii, T. A. Denidni, and A. Gharsallah, "Beam-switching antenna with a new reconfigurable frequency selective surface," *IEEE Antennas Wireless Propag. Lett.*, vol. 15, pp. 1159–1162, 2016.
[10] H. A. Rahman and S. K. A. Rahim, "Dual band PDMS based flexible antenna for wearable application," in *Proc. IEEE MTT-S Int. Microw. Workshop Ser. RF Wireless Technol. Biomed. Healthcare Appl. (IMWS-BIO)*, Sep. 2015, vol. 1. no. 1, pp. 193–194.
[11] L. Matekovits, J. Huang, I. Peter, and K. P. Esselle, "Mutual coupling reduction between implanted microstrip antennas on a cylindrical bio-metallic ground plane," *IEEE Access*, vol. 5, pp. 8804–8811, 2017.
[12] S. A. Babale, S. K. A. Rahim, M. Jusoh, and L. Zahid, "Branch-line coupler using PDMS and Shieldit Super fabric conductor," *Appl. Phys. A, Solids Surf.*, vol. 123, no. 2, p. 117, 2017. [Online]. Available: http://link.springer.com/10.1007/s00339-016-0617-3
[13] H. A. Rahman, S. K. A. Rahim, M. Abedian, and N. Najib, "Design of a flexible antenna using printed silver loaded epoxy on PDMS/plastic substrate for wearable applications," in *Proc. 10th Eur. Conf. Antennas Propag. (EuCAP)*, 2016, pp. 1–4.
[14] S. Kim *et al.*, "Inkjet-printed antennas, sensors and circuits on paper substrate," *IET Microw. Antennas Propag.*, vol. 7, no. 10, pp. 858–868, Jul. 2013. [Online]. Available: http://digital-library.theiet.org/content/journals/10.1049/iet-map.2012.0685
[15] (2014). *Datasheet: AgIC Ink 1000*. [Online]. Available: https://agic.cc/en
[16] W. Xin-Lei, Y. Yan-Ling, Z. De-Hua, X. Wei, C. Yi-Feng, and C. Yu, "Design and modelling of the cylindrical conformal FSS with mechanical bending cover method," *Procedia Comput. Sci.*, vol. 107, pp. 824–829, 2017.

WAI YAN YONG received the Bachelor's degree (Hons.) in electronic engineering from Universiti Tun Hussein Onn Malaysia in 2016. He is currently pursuing the Master's degree with the Wireless Communication Center, Universiti Teknologi Malaysia. His research interests include but not limited to electromagnetic compatibility, metamaterial absorbers, conformal microwave devices, and electromagnetic for biomedical applications.

SHARUL KAMAL ABDUL RAHIM received the degree in electrical engineering from The University of Tennessee, USA, the M.Sc. degree in engineering (communication engineering) from Universiti Teknologi Malaysia (UTM), and the Ph.D. degree in wireless communication system from the University of Birmingham, U.K., in 2007. After his graduation from The University of Tennessee, he spent three years in industry. After graduating the M.Sc. degree, he joined UTM in 2001, where he is currently a Professor with the Wireless Communication Centre. He has published over 200 learned papers, including an the *IEEE Antenna and Propagation Magazine*, the IEEE TRANSACTIONS ON ANTENNA AND PROPAGATION, the IEEE ANTENNA AND PROPAGATION LETTERS, and taken various patents. His research interests include antenna design, smart antenna system, beamforming network, and microwave devices for fifth generation mobile communication. He is a Senior Member of IEEE Malaysia Section, a member of the Institute of Engineer Malaysia, a Professional Engineer with BEM, a member of the Eta Kappa Nu Chapter, University of Tennessee, and the International Electrical Engineering Honor Society. He is currently an Executive Committee of the IEM Southern Branch.

MOHAMED HIMDI received the Ph.D. degree in signal processing and telecommunications from the University of Rennes 1, Rennes, France, in 1990. Since 2003, he has been a Professor with the University of Rennes 1, and the Head of the High Frequency and Antenna Department, Institute d'Electronique et Telecommunications de Rennes, until 2013. He has authored or co-authored 110 journal papers, over 250 papers in conference proceedings, and nine book chapters. He holds 38 patents in the area of antennas. His research interests include passive and active millimeter-wave antenna, theoretical and applied computational electromagnetics, development of new architectures of printed antenna arrays, and new 3-D antenna technologies. He was a recipient of the International Symposium on Antennas and Propagation Conference Young Researcher Scientist Fellowship, Japan, in 1992 and an award was presented by the International Union of Radio Scientist, Russia, in 1995. He was a Laureate of the Second National Competition for the Creation of Innovative Company, Ministry of Industry and Education, France, in 2000 and 2015. In 2015, he received the JEC-AWARD-10 at Paris on Pure composite material antenna embedded into a motorhome roof for the Digital Terrestrial Television reception.

FAUZIAHANIM CHE SEMAN (M'14) received the degree in electrical communication engineering from Universiti Teknologi Malaysia in 2001, the master's degree from Universiti Tun Hussein Onn Malaysia in 2003, and the Ph.D. degree from the Queen's University of Belfast, U.K., in 2011. After the Master's degree, she joined the Faculty of Electrical Engineering, Universiti Tun Hussein Onn Malaysia as a Lecturer, where she is currently an Associate Professor with the Research Center of Applied Electromagnetic. She has published number of index journals and conference proceedings and taken various patents. Her research interests include radar microwave absorber, frequency selective surface, antenna design, and copper access networks. She is a Senior Member of BEM. She also involved in the organizing committee for various conferences, such as the Technical Chair for the IEEE APMC 2017. She is currently the Chairman of IEEE AP/MTT/EMC Malaysia Section.

DING LIK SUONG received the B.E. degree (Hons.) in mechatronics, robotics, and automation engineering from Manchester Metropolitan University. He is currently pursuing the Ph.D. degree with the Research Center of Applied Electromagnetic, Universiti Tun Hussein Onn Malaysia. Since 2014, he has been with RF Station Sdn Bhd as a Sales and Application Engineer. His research interests include electromagnetic compatibility and antenna and propagation.

MUHAMMAD RIDDUAN RAMLI was born in Kuala Terengganu, Malaysia. He received the degree in electrical (electronic) engineering in 2015. He is currently pursuing the Master's degree with the Wireless Communication Centre, Faculty of Electrical Engineering, Universiti Teknologi Malaysia, Johor Bahru, Malaysia.

HUSAMELDIN ABDELRAHMAN ELMOBARAK received the degree in electrical and electronic engineering (communication engineering) and the M.Sc. degree from the University of Khartoum, Sudan, in 2002 and 2008, respectively, and the Ph.D. degree with the Wireless Communication Centre, Faculty of Electrical Engineering, Universiti Teknologi Malaysia, Johor Bahru, Malaysia. His research interests include flexible and conformal antenna applications.